ARTICLE

A Selective Fluorescent Sensing of $H_2PO_4^-$ by the Formation of Anion Induced Self-Assembly Supramolecular Polymer †

Received 00th January 20xx,
Accepted 00th January 20xx

DOI: 10.1039/x0xx00000x

Paula Sabater,[a] Fabiola Zapata,*[a] Adolfo Bastida,[b] Antonio Caballero*[a]

The utilization of anions to induce the formation of self-assembled supramolecular polymers in solution is an undeveloped area of host–guest chemistry. We report in this manuscript a comparative study of two tripodal anion receptors by hydrogen or halogen bonding interactions to form self-assembly supramolecular structures induced by the presence of anions. DOSY NMR and DLS experiments provided evidence for the formation of supramolecular structures in solution in both halogen and hydrogen bond donor with $H_2PO_4^-$ anion. The nucleation and elongation constants obtained by the thermodynamic model indicate that the polymers grow following an isodesmic mechanism. Emission studies demonstrate that only the formation of the supramolecular polymer between halogen bond donor receptor and $H_2PO_4^-$ anions results in the apparition of the excimer emission band.

Introduction

Anion coordination is an important issue in supramolecular chemistry. Despite the progress done in the past two decades, this research field continues being one of the most active within the supramolecular chemistry research field and therefore a considerable number of new anion receptors are reported each year.[1-8] Anion receptors are designed to selectively recognize anionic species, the selectivity mostly depends upon size and shape complementarity between the receptor and the anion. In general, the most employed anion receptors are those with a preorganised and rigid structure because of the energy of the interaction is intrinsically low and a cage-shaped system can afford additional stability to the receptor–anion complex.[9]

The most popular non-covalent interaction used for anion recognition has been hydrogen bond.[10-16] Very recently, the utilization of other elements belonging to groups 14 to 17 have been used in the anion recognition field[17-22] due to the presence of a positive charge region so-called σ-hole. The origin of the attraction is caused by the anisotropy of the electronic density in the atoms where regions of positive (σ-holes) and negative (σ-lumps) electron density are originated.[23,24] Between the atoms which present σ–holes, halogen atoms have undoubtedly been the most explored and a remarkable number of examples have been described.[25-30]

In the last years, the interest in the development of new supramolecular architectures through the self-assembly of two or more molecular components using non-covalent interactions has grown tremendously. Despite the successful utilization of cation as a template of complicated supramolecular aggregation or supramolecular polymer,[31-42] the use of anions is much less explored, even taking into account that the utilization of anions is highly interesting due to their wider range of geometries and therefore, the self-assembled architectures formed could be different by varying the geometry of the anions involved in a self-assembly process. The formation of anion induced supramolecular capsules constitutes some of the few examples described in which the anions have been used in the construction of supramolecular aggregates in solution.[43-52]

Recently, the research interests of our group have moved from the synthesis of selective anion receptors or sensor by a discrete anion-receptor complexes towards the formation of anion induced supramolecular polymers.[53] Here we describe a comparative study of the ability to form self-assembly supramolecular structures induced by the presence of anions between two tripodal anion receptors by hydrogen or halogen bonding interactions. Traditionally, the utilization of tripodal molecules has been widely employed in the construction of anion receptors where the three arms are orientated in the same direction adopting a cone conformation to bind the anion.[54-63]

Herein, we have designed a benzene scaffold based 2-H-imidazolium or 2-Br-imidazolium substituted tripodal HB and XB donor receptor respectively end-capped with anthracene groups not only with a fluorescent anion sensing purposed but also as a bulky group to favour the formation of supramolecular structures instead of the cone conformation.

Results and discussion

The tris-imidazolium receptors $\mathbf{6^{3+}\cdot 3PF_6^-}$ and $\mathbf{7^{3+}\cdot 3PF_6^-}$ were prepared by a stepwise procedure which involves the initial reaction of 1,3,5-tris(bromomethyl)-2,4,6-Triethylbenzene **1** with 2-bromo-4,5-dimethyl-1*H*-imidazole **2**[64] or 4,5-dimethyl-

[a] Departamento de Química Orgánica, Universidad de Murcia, Campus de Espinardo, 30100 Murcia, Spain. E-mail: antocaba@um.es, fazafer@um.es.
[b] Departamento de Química Física, Universidad de Murcia, Campus de Espinardo, 30100 Murcia, Spain.

† Electronic supplementary information (ESI) available: NMR spectra, fluorescence and ^{1}H-NMR anion binding studies. See DOI: 10.1039/x0xx00000x

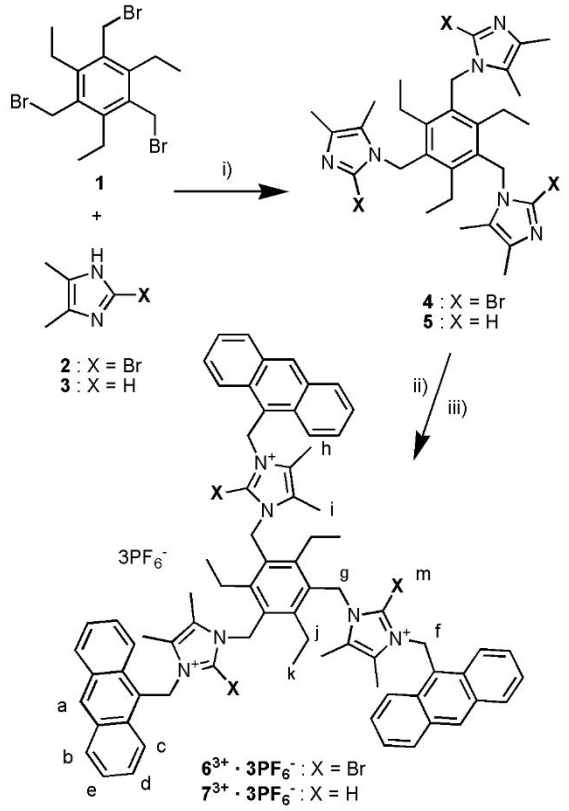

Scheme 1. Synthesis of the Halogen and Hydrogen-Bonding Tris-Imidazolium Receptors $\mathbf{6^{3+}\cdot 3PF_6^-}$ and $\mathbf{7^{3+}\cdot 3PF_6^-}$. Reagents and conditions: (i) NaOH (1M in H_2O), CH_3CN, RT; (ii) 9-(bromomethyl)anthracene, CH_3CN, RT; (iii) NH_4PF_6 in H_2O.

1*H*-imidazole **3**[65] in acetonitrile in the presence of NaOH to give the corresponding tris-imidazoles **4** and **5** respectively. A subsequent alquilation reaction of **4** or **5** with 9-(bromomethyl) anthracene afforded the halogen- or hydrogen-bonding tris-imidazolium receptors as bromide salts in 42% and 36% yield respectively. The desired receptors as PF_6^- salt $\mathbf{6^{3+}\cdot 3PF_6^-}$ and $\mathbf{7^{3+}\cdot 3PF_6^-}$ were obtained in quantitative yield by several washings with aqueous solution of NH_4PF_6 (Scheme 1). The new compounds were fully characterized using standard techniques: ^{1}H NMR, ^{13}C NMR and FAB mass spectrometry.

Anion binding studies

The anion binding properties of the halogen- and hydrogen-bonding receptors $\mathbf{6^{3+}\cdot 3PF_6^-}$ and $\mathbf{7^{3+}\cdot 3PF_6^-}$ toward $HP_2O_7^{3-}$, $H_2PO_4^-$, SO_4^{2-}, HSO_4^-, NO_3^-, F^-, Cl^-, Br^-, I^-, $CH_3CO_2^-$, $C_6H_5CO_2^-$, ClO_4^- and BF_4^- as tetrabutylammoium salts, were initially investigated using ^{1}H NMR titration experiments through the addition of different anions to solutions of the receptors in CD_3CN/CD_3OD (8:2 v/v). Halogen and hydrogen bond donor receptors $\mathbf{6^{3+}\cdot 3PF_6^-}$ and $\mathbf{7^{3+}\cdot 3PF_6^-}$ respectively have similar ^{1}H NMR spectra in CD_3CN/CD_3OD (8:2 v/v). The only exception is the presence of the imidazolium proton H_m at δ = 6.37 ppm in the bis-imidazolium receptor $\mathbf{7^{3+}\cdot 3PF_6^-}$, which is obviously absent in the bis-bromoimidazolium receptor $\mathbf{6^{3+}\cdot 3PF_6^-}$. Both receptors show the same set of signals: the protons of the ethyl group H_j and H_k linked to the benzene spacer unit appear in the aliphatic region in the range δ = 0.15–2.44 ppm, the methyl protons H_h and H_i located at the imidazolium rings appear at δ = 1.72-2.48 ppm and the protons of the two methylenes attributed to the fragments benzene–CH_2–imidazolium (H_g) and imidazolium–CH_2–anthracene (H_f) appear as two different singlets around δ 4.49–6.36 ppm, finally the anthracene protons (H_a, H_b, H_c, H_d and H_e) appear in the aromatic region.

The addition of an increasing amounts of SO_4^{2-} (Figure 1), $HP_2O_7^{3-}$, and $H_2PO_4^-$ anions to different solutions of the receptor $\mathbf{7^{3+}\cdot 3PF_6^-}$ in CD_3CN/CD_3OD (8:2 v/v) shows the typical behaviour of the formation of anion-receptor complex by hydrogen bonding interaction. Thus, the signal attributed to the imidazolium proton H_m was the most affected, which was downfield shifted $\Delta\delta$ = 1.34 ppm when $H_2PO_4^-$ was added, indicating a direct interaction with the anion by hydrogen bond. Unfortunately, this signal gradually disappeared during the addition of SO_4^{2-} and $HP_2O_7^{3-}$ anions probably due to an acid-base equilibrium with the deuterium of the solvent. Surprisingly an important downfield shift in the resonance of the ethylene protons H_k ($\Delta\delta$ = 1.08 – 0.35 ppm) was also observed as well as in the methylene protons H_g and H_f $\Delta\delta$ = 0.77 – 0.31 ppm and $\Delta\delta$ = 0.75 – 0.18 ppm respectively. On contrary, resonance of the methyl proton H_d was upfield shifted ($\Delta\delta$ = –1.11 – –0.26 ppm).

The behaviour observed in the ^{1}H NMR experiment during the addition of the previously mentioned set of anions to a solution of the halogen bond donor receptor $\mathbf{6^{3+}\cdot 3PF_6^-}$ was remarkably different to the discussed previously for the receptor $\mathbf{7^{3+}\cdot 3PF_6^-}$. In this case, the presence of $HP_2O_7^{3-}$, SO_4^{2-} or F^- anions in a solution of the receptor $\mathbf{6^{3+}\cdot 3PF_6^-}$ promotes the disappearance of the resonances attributed to the receptor and the apparition of new signals (see the ESI S5–S7†). Mass spectrometry experiments indicate that the presence of $HP_2O_7^{3-}$, SO_4^{2-} and F^- produce the conversion of the Tris(2-bromoimidazolium) $\mathbf{6^{3+}\cdot 3PF_6^-}$ into the Tris(2-imidazolone) (see the ESI S8–S9†) which is in concordance which previously results described by our research group.[29]

The titration profile obtained after the addition of $H_2PO_4^-$ to a solution of the halogen bonding receptor $\mathbf{6^{3+}\cdot 3PF_6^-}$ in

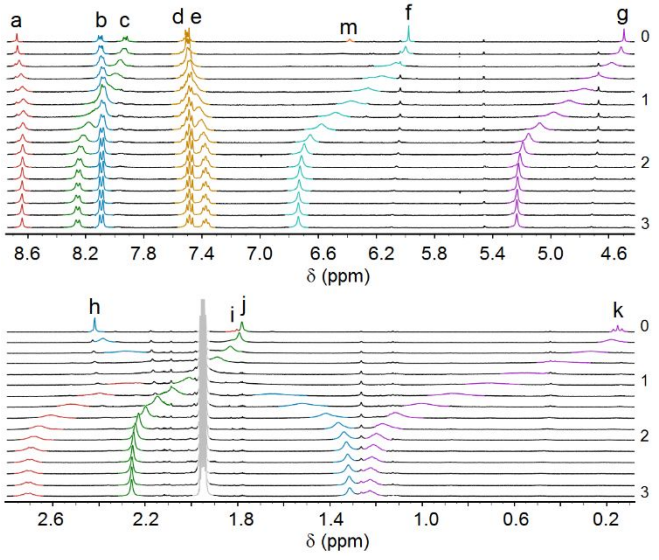

Figure 1. ^{1}H NMR spectral changes observed in the receptor $\mathbf{7^{3+}\cdot 3PF_6^-}$ in CD_3CN/CD_3OD (8:2 v/v) during the addition of up to 3 equiv of SO_4^{2-} anions.

CD_3CN/CD_3OD (8:2 v/v) (see the ESI S10†) showed a critical transition point when 0.6 equiv of the anion was added. The addition of up 0.6 equiv of $H_2PO_4^-$ did not promote any changes in the ^1H NMR spectra of the receptor **$6^{3+}\cdot 3PF_6^-$**, but subsequent additions promoted a downfield shift of the H_f ($\Delta\delta$ = 0.01 ppm), H_g ($\Delta\delta$ = 0.07 ppm), and H_c ($\Delta\delta$ = 0.04 ppm) protons. This behaviour suggests a polymerization process rather than the typical recognition event.[66]

The addition of HSO_4^-, NO_3^-, Cl^-, Br^-, I^-, $CH_3CO_2^-$, $C_6H_5CO_2^-$, ClO_4^- and BF_4^- to a solution of the receptor **$6^{3+}\cdot 3PF_6^-$** or **$7^{3+}\cdot 3PF_6^-$** did not show remarkable perturbation in their ^1H NMR spectra. In order to distinguish between the formation of the self-assembly supramolecular polymers and the formation of the classical anion-receptor recognition process, diffusion NMR experiments (DOSY-NMR) and dynamic light scattering (DLS) studies were carried out.

The results obtained by DOSY NMR shown a significant decrease in the diffusion coefficient (D) of the receptors **$6^{3+}\cdot 3PF_6^-$** (ΔD = −17%) and **$7^{3+}\cdot 3PF_6^-$** (ΔD = −21%) (c = 4·10^{-3} M in CD_3CN/CD_3OD 8:2 v/v) when $H_2PO_4^-$ anions are present which is attributed to the formation of supramolecular structures. Interestingly, the presence of SO_4^{2-} or $HP_2O_7^{3-}$ anions did not cause remarkable perturbation in the diffusion coefficient of the receptors **$6^{3+}\cdot 3PF_6^-$** and **$7^{3+}\cdot 3PF_6^-$** (Table 1). Additional evidences of the formation of the supramolecular structures in solution induces by the presence of $H_2PO_4^-$ anions were also obtained by DOSY NMR, where a clear dependence of the diffusion coefficients of the supramolecular species with the concentration was observed, therefore, a gradual decrease in D was obtained when the concentration of the **$6^{3+}\cdot 3PF_6^-$** and **$7^{3+}\cdot 3PF_6^-$** was increased, which is consistent with the formation of self-assembled supramolecular structures. In contrast, the diffusion coefficients D of the receptors remained practically unperturbed at different concentrations (Table 1), indicating no aggregation of the receptor in the absence of anions.

Table 1 Diffusion coefficients values of **$6^{3+}\cdot 3PF_6^-$**, **$7^{3+}\cdot 3PF_6^-$** and complex formed with different anions in CD_3CN/CD_3OD (8:2 v/v). The variation of the diffusion coefficients in percentage is shown in parenthesis

Complex	D·10^{10} (%D)		
	8·10^{-4} M	2·10^{-3} M	4·10^{-3} M
$6^{3+}\cdot 3PF_6^-$	7.685	7.816	7.953
$6^{3+}\cdot 3PF_6^-$+$H_2PO_4^-$	7.492 (-2.5)	6.983 (-10.7)	6.651 (-17.2)
$7^{3+}\cdot PF_6^-$	7.542	8.005	8.358
$7^{3+}\cdot PF_6^-$+$H_2PO_4^-$	7.330 (-2.8)	7.245 (-9.5)	6.636 (-20.6)
7^{3+} PF_6^-+$HP_2O_7^{3-}$	8.252 (5.1)	7.511 (-7.9)	7.802 (-5.2)
$7^{3+}\cdot$ PF_6^-+SO_4^{2-}	8.529 (3.3)	8.211 (0.6)	8.108 (-0.9)

DLS measurements at different concentrations (c = 5·10^{-6} M and 1·10^{-5} M) were performed to determine the size of the supramolecular polymers in CH_3CN. The values of the hydrodynamic diameter of the species formed after the addition of $H_2PO_4^-$ to a solution of **$6^{3+}\cdot 3PF_6^-$** were d_H (c = 5·10^{-6} M) = 113 and d_H (c = 1·10^{-5} M) =227 nm and d_H (c = 5·10^{-6} M) = 97 and d_H (c = 1·10^{-5} M) = 182 nm for **$7^{3+}\cdot 3PF_6^-$**. As expected for this kind of supramolecular structures, a decrease of the hydrodynamic diameter with decreasing concentration was observed (Figure 2). These results are in good agreement with the DOSY NMR results discussed previously.

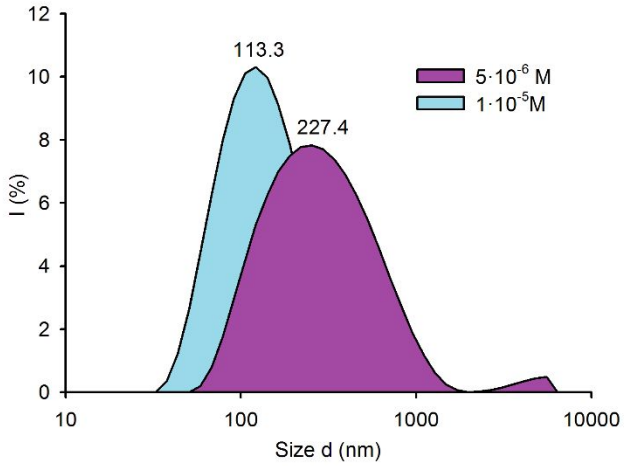

Figure 2. Distribution of the hydrodynamic diameter of **$6^{3+}\cdot 3PF_6^-$ +$H_2PO_4^-$** as measured though DLS at c = 5·10^{-6} (blue) and 1·10^{-5} M (purple) in CH_3CN at 25°C.

In a recent paper[53] we have shown that the NMR shifts of supramolecular polymers can be accurately described using a cooperative polymerization model, which is characterized by two equilibrium constants K_N and K_E corresponding to the nucleation and elongation steps described by the following chemical equilibria

$$A + nB \rightleftarrows (AB_n),\ K_N = \frac{[(AB_n)]}{[A][B]^n} (\mathrm{M}^{-n}) \ (\mathbf{1})$$

$$(AB_n) + A + nB \rightleftarrows (AB_n)_2,\ K_E = \frac{[(AB_n)_2]}{[(AB_n)][A][B]^n} (\mathrm{M}^{-1-n}) \ (\mathbf{2})$$

$$(AB_n)_{i-1} + A + nB \rightleftarrows (AB_n)_i,\ K_E = \frac{[(AB_n)_i]}{[(AB_n)_{i-1}][A][B]^n} (\mathrm{M}^{-1-n}) \ (\mathbf{3})$$

where A, B and $(AB)_i$ denote the receptor, the anion, and the supramolecular polymer of length i respectively. In the initial nucleation step (1) an (AB_n) nucleus is formed which is subsequently elongated through the reversible addition of the monomers to post-nucleus polymer. We note that the above equations generalize our previous model by considering now a polymer with general n:1 anion-receptor stoichiometry. From these equations it is straightforward to derive the following expressions relating the total concentrations of A and B in the experiments (C_A and C_B) and their concentrations at equilibrium ([A] and [B])

$$C_A = [A] + K_N \frac{[A][B]^n}{(1 - K_E[A][B]^n)^2} \ (\mathbf{4})$$

$$C_B = [B] + nK_N \frac{[A][B]^n}{(1 - K_E[A][B]^n)^2} \quad (5)$$

The [A] concentrations can be estimated from the measured NMR shifts, assuming that they can be evaluated using the following weighted sum:

$$\delta = \frac{[A]}{C_A}\delta_A + \frac{C_A - [A]}{C_A}\delta_{sp} \quad (6)$$

where δ_A and δ_{sp} are the NMR shifts in the isolated receptor and the supramolecular polymer, respectively. The values of K_N, K_E, and δ_{sp} are fitted using equations (4)-(6) to reproduce the observed NMR shifts as shown in Figure 3. In a first sets of fits the *n* stoichiometric coefficient was also considered as a fitting parameter providing the values 2.16 and 1.85 for the **6·$^{3+}$·2$H_2PO_4^-$** and **7·$^{3+}$·2$H_2PO_4^-$** polymers respectively what provides an additional confirmation of their 2:1 stoichiometry. In the second sets of fits the value of *n* was fixed to 2 providing $K_N = 3.2 \cdot 10^4$ M^{-2} and $K_E = 3.5 \cdot 10^6$ M^{-3} for **6·$^{3+}$·2$H_2PO_4^-$** and $K_N = 6.7 \cdot 10^4$ M^{-2} and $K_E = 2.0 \cdot 10^7$ M^{-3} for **7·$^{3+}$·2$H_2PO_4^-$** . Although both equilibrium constants have different units, we can estimate their similarity using the value of C_A as a conversion factor. In that case we obtain values of K_N and $K_E \cdot C_A$ which differ in less than order of magnitude what indicates that the nucleation and elongation processes are of similar thermodynamic magnitude what explains the isodesmic profiles[66-67] of the NMR shifts observed in Figure 3.

The association constants of the traditional anion-receptor complexes formed between the receptor **7^{3+}·3PF_6^-** with SO_4^{2-} and $HP_2O_7^{3-}$ were obtained by fitting the ^{1}H NMR titration data to the calculated anion-receptor stoichiometry from the Job´s plot experiments (see the ESI S3†) by using Dynafit program[68] and are collected in Table 2.

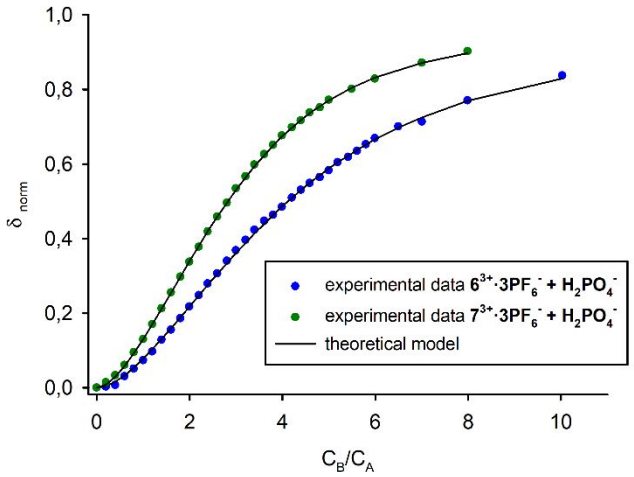

Figure 3. Normalized NMR shifts ($\delta_{norm}=(\delta_{obs}-\delta_A)/(\delta_{sp}-\delta_A)$). Points correspond to the experimental measurements and lines to the fit to the thermodynamic mechanism proposed

Table 2. Association constants calculated by ^{1}H NMR for receptor **7^{3+}·3PF_6^-** with $HP_2O_7^{3-}$ and SO_4^{2-} anions in CD_3CN/CD_3OD (8:2 v/v). Errors (in percent) are given in parenthesis

	Anion-receptor stoichiometry	*K* (M^{-1})
7^{3+}·3PF_6^- + $HP_2O_7^{3-}$	1:1	$1.2 \cdot 10^4$ (7%)
7^{3+}·3PF_6^- + SO_4^{2-}	2:1	$K_1 = 3.5 \cdot 10^4$ (15%) $K_2 = 2.7 \cdot 10^4$ (12%)

A highly directional needles were obtained after the addition of $H_2PO_4^-$ to a solution of receptor **7^{3+}·3PF_6^-**. The stereomicroscope image of the crystals revealed the formation of a monodimensional crystal structures formed by yellow needles which seem to grow from the same centre, extending in sphere shaped (Figure 4). Unfortunately, all the crystals obtained were extremely weakly diffracting and therefore it was not possible to obtain the X ray structures of the supramolecular polymer formed.

Anion sensing studies

Figure 4. Stereomicroscope images of the self-assembled compound **7^{3+}·2$H_2PO_4^-$**.

The sensing properties of the receptors $\mathbf{6^{3+}\cdot 3PF_6^-}$ and $\mathbf{7^{3+}\cdot 3PF_6^-}$ were also investigated by UV-vis and fluorescence spectroscopies in CH_3CN by stepwise addition of increasing amounts of the previously mentioned set of anions. The UV-vis spectra of the receptors $\mathbf{6^{3+}\cdot 3PF_6^-}$ and $\mathbf{7^{3+}\cdot 3PF_6^-}$ in CH_3CN are very similar, both present two intense absorption bands around λ = 210 and 255 nm, along with the characteristic absorption bands attributed to the anthracene moieties at λ = 335, 353, 370, and 390 nm.

The addition of increasing amounts of the previously mentioned set of anions did not promote remarkable perturbation in the UV-vis spectrum of the hydrogen bond donor receptor $\mathbf{7^{2+}\cdot 2PF_6^-}$ ($c = 1 \times 10^{-5}$M in CH_3CN). On contrary, the presence of $HP_2O_7^{3-}$, $H_2PO_4^-$, SO_4^{2-}, and F^- anions to a solution of the halogen bond donor $\mathbf{6^{2+}\cdot 2PF_6^-}$ ($c = 1 \times 10^{-5}$M in CH_3CN) induced important perturbations in the absorption spectrum of the receptor. The addition of those anions causes two different effects. First, the presence of $H_2PO_4^-$ anions, which induces the formation of supramolecular structures, promotes the decrease in the high-energy bands at λ 230 and 255 nm while the anthracene

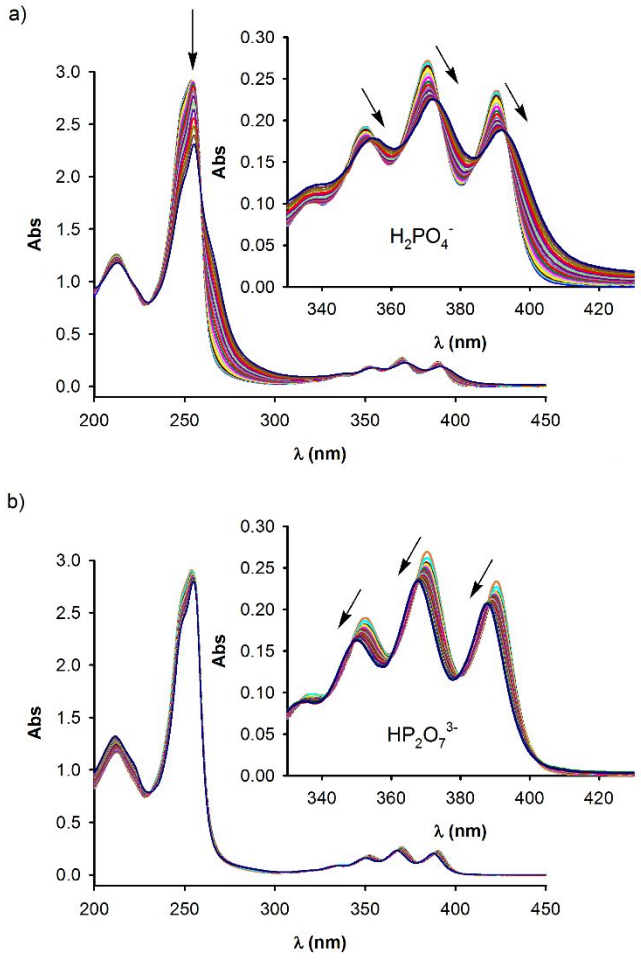

Figure 5. Changes in the absorption spectra of the receptor $\mathbf{6^{3+}\cdot 3PF_6^-}$ ($c = 1 \times 10^{-5}$ M in CH_3CN) upon addition of increasing amounts of (a) $H_2PO_4^-$ and (b) $HP_2O_7^{3-}$ anions. Arrows indicate the absorption bands that increase or decrease during the titration.

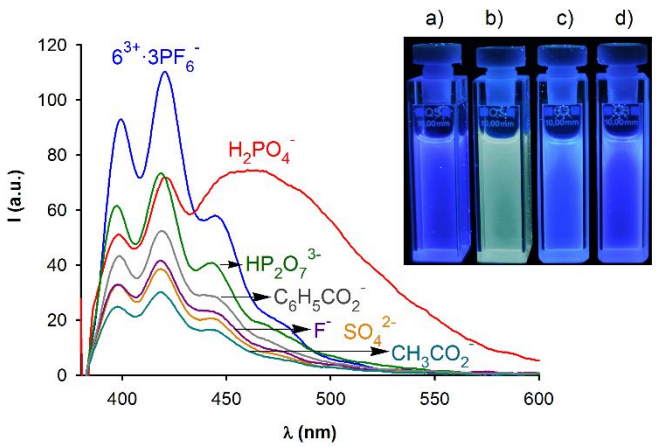

Figure 6. Emission spectra of the receptor $\mathbf{6^{3+}\cdot 3PF_6^-}$ ($c = 5\cdot 10^{-6}$ M in CH_3CN) (blue line) after the addition of excess of $H_2PO_4^-$ (red line), SO_4^{2-} (orange line), F^- (violet line), $HP_2O_7^{3-}$ (green line), $CH_3CO_2^-$ (turquoise line) and $C_6H_5CO_2^-$ (grey line). Inset: visual changes in the fluorescence of receptor $\mathbf{6^{3+}\cdot 3PF_6^-}$ (a) upon the addition of (b) $H_2PO_4^-$, (c) SO_4^{2-} and (d) $HP_2O_7^{3-}$.

absorption bands were red-shifted by Δλ = 2 nm, several well-defined isosbestic points at λ = 332, 359, 340, 355, 370, 390, 441 and 448 nm were also observed during the titration process (Figure 5a). Second, $HP_2O_7^{3-}$, SO_4^{2-}, and F^- anions, which cause the formation of the imidazolone ring, did not modify the high-energy bands at λ 210 and 255 nm, while the anthracene absorption bands at 335, 353, 370, and 390 nm were blue-shifted by Δλ = -2 nm (Figure 5b).

The emission spectra of the receptors $\mathbf{6^{3+}\cdot 3PF_6^-}$ and $\mathbf{7^{3+}\cdot 3PF_6^-}$ in CH_3CN using an excitation wavelength of 370 nm exhibit only the characteristic anthracene monomeric emission bands around λ = 399, 420 and 445 nm. The quantum yield of the hydrogen bond donor $\mathbf{7^{3+}\cdot 3PF_6^-}$ ($\Phi = 0.59$) is almost 72 times higher than the halogen bond donor $\mathbf{6^{3+}\cdot 3PF_6^-}$ ($\Phi = 0.0082$), the decrease of the quantum yield in the halogenated compound $\mathbf{6^{3+}\cdot 3PF_6^-}$ could be probably attributed to an intramolecular heavy-atom effect caused by the bromine atoms present in the receptor.[69-71]

The addition of $HP_2O_7^{3-}$, SO_4^{2-}, F^-, $CH_3CO_2^-$ and $C_6H_5CO_2^-$ anions promotes a remarkable decrease in the monomer emission bands of both receptors $\mathbf{6^{3+}\cdot 3PF_6^-}$ and $\mathbf{7^{3+}\cdot 3PF_6^-}$. Interestingly, while the presence of $H_2PO_4^-$ anions in a solution of the hydrogen bond donor $\mathbf{7^{3+}\cdot 3PF_6^-}$ also cause decrease in the emission intensity of monomer bands, the addition of $H_2PO_4^-$ anions to a solution of the halogen bond donor $\mathbf{6^{3+}\cdot 3PF_6^-}$ promotes a progressive increase of a new broad emission band at λ = 469 nm, assigned to the anthracene excimer emission band, with a concomitant decrease in the monomer emission bands at λ = 399, 420 and 445 nm (Figure 6). The selective detection of $H_2PO_4^-$ anion can be observed by the naked eye due it is the only anion which cause a yellow emission (Figure 6 inset)

Taking into account the following aspects: 1.- the 2:1 anion/receptor stoichiometry obtained in the case of the $H_2PO_4^-$ anions using the theoretical model. 2.- The tendency of the

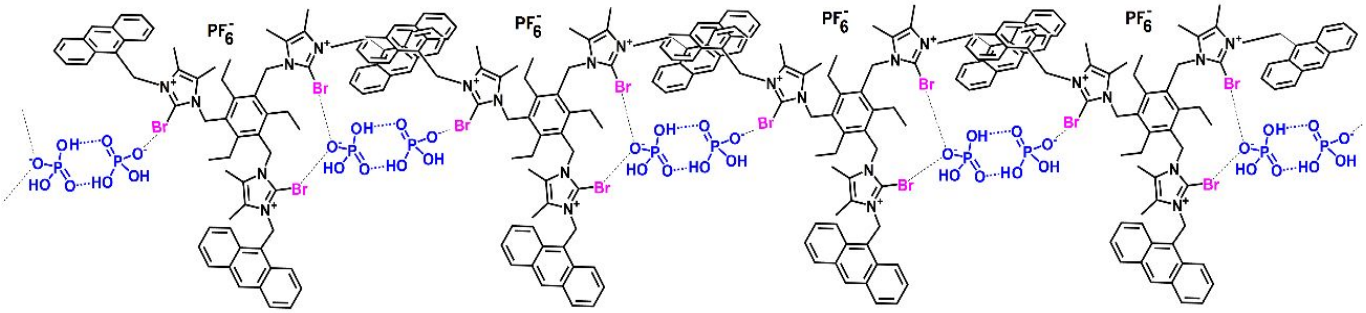

Figure 7. Proposed structure of the supramolecular polymer formed between the receptor $\mathbf{6^{3+}{\cdot}3PF_6^-}$ and the $H_2PO_4^-$ anion.

$H_2PO_4^-$ anion to form dimers.[72-74] 3.- The formation of supramolecular structures detected by DOSY NMR and DLS when $H_2PO_4^-$ anions are added to a solution of the receptor $\mathbf{6^{3+}{\cdot}3PF_6^-}$ and finally, 4.- The formation of the anthracene excimer in the receptor $\mathbf{6^{3+}{\cdot}3PF_6^-}$ with the presence of $H_2PO_4^-$. We propose the formation of the supramolecular polymer induced by the $H_2PO_4^-$ anion shown in Figure 7.

The structure of the supramolecular polymer formed between the receptor $\mathbf{7^{3+}{\cdot}3PF_6^-}$ and the $H_2PO_4^-$ anion should be slightly different due to the excimer emission of the anthracene was not observed.

Conclusion

In conclusion, the hydrogen bond donor anions receptor $\mathbf{7^{3+}{\cdot}3PF_6^-}$ shows two different anion binding modes. ^{1}H NMR, DOSY NMR and DLS experiment indicate the formation of the traditional anion-receptor complexes with $HP_2O_7^{3-}$ and SO_4^{2-} anions while the formation of supramolecular polymers were detected only with the presence of $H_2PO_4^-$ anions. The formation of those supramolecular polymer induced by the $H_2PO_4^-$ anion were also detected in the halogen bond donor $\mathbf{6^{3+}{\cdot}3PF_6^-}$. The nucleation and elongation constants obtained by the thermodynamic model indicate that the polymers grown following an isodesmic mechanism. $HP_2O_7^{3-}$, SO_4^{2-} and F^- produce a chemical reaction in the receptor $\mathbf{6^{3+}{\cdot}3PF_6^-}$ where the bromo-imidazolium rings are converted in the 2-imidazolone rings. Remarkably, emission studies demonstrate that only the formation of the supramolecular polymer between $\mathbf{6^{3+}{\cdot}3PF_6^-}$ and $H_2PO_4^-$ anions results in the apparition of the excimer emission band which is a very interesting and novel mechanism for the selective anion sensing.

Experimental Section

General Comments

All reactions were carried out using solvents that were dried by routine procedures. All melting points were determined by means of a Kofler hot-plate melting-point apparatus and are uncorrected. Solution ^{1}H, and ^{13}C NMR spectra were recorded at 200, 300, 400, or 600 MHz. The following abbreviations have been used to state the multiplicity of the signals: s (singlet), d (doublet), dd (double doublet), t (triplet), m (multiplet). Chemical shifts (δ) in the ^{1}H and ^{13}C NMR spectra are referenced to tetramethyl silane (TMS). Diffusion NMR experiments (DOSY) were recorded with a Bruker 600 spectrometer (^{1}H) using the LED-BPP sequence with a diffusion period (Δ) of 150 ms, field gradient pulses (δ) of 4 ms applied as half-sine profile bipolar pairs and an LED period of 5 ms. Field gradients were varied from 2-90% of maximum (53 G/cm) in 16 steps and data were analysed using Bruker TOPSPIN 2.1 software. UV-Vis and fluorescence spectra were carried out in the solvents and concentrations stated in the text and in the corresponding figure captions, using a dissolution cell with 10 mm path length, and they were recorded with the spectra background corrected before and after sequential additions of different aliquots of anions. Quantum yield values were measured with respect to anthracene as the standard ($\Phi = 0.27 \pm 0.01$) using the equation $\Phi_x/\Phi_s = (S_x/S_s)\ [(1 - 10^{-As})/(1 - 10^{-Ax})](n_s^2/n_x^2)$, where x and s indicate the unknown and standard solution, respectively, Φ is the quantum yield, S is the area under the emission curve, A is the absorbance at the excitation wavelength and n is the refractive index. Mass spectra were recorded with 3-nitrobenzylalcohol as a matrix.

Dynamic Light Scattering analyses were performed using a Malvern Zetasizer Nano ZS (Malvern Instruments Ltd, UK) at 25°C and a 173° angle relative to the source. The hydrodynamic diameter distributions were obtained by volume using the software package of the apparatus. Each curve represents the average of 3 measurements (16 runs each). Prior to analysis, all solutions were filtered.

Stereomicroscope image was obtained using a Leica 76 APO stereomicroscope connected to a Leica DC500 digital camera and Software CombineZM. The crystals were placed on a cover glass. The crystals were obtained by the vapour diffusion of diethyl ether into a solution of the receptors and $H_2PO_4^-$ anion in $CH_3CN/CH_3OH/^iPrOH$.

Synthesis

Synthesis of 1,3,5-tris((2-bromo-4,5-dimethylimidazol-1-yl)methyl)-2,4,6-Triethylbenzene 4. (0.339 g, 80%) To a solution of 2-bromo-4,5-trimethyl-1*H*-imidazole **2** (0.334 g, 1.9 mmol) in acetonitrile (20 ml) was added dropwise a solution of 1 M NaOH (1.9 mmol), and the solution was stirred for 10 min. The 1,3,5-tris(bromomethyl)-2,4,6-triethylbenzene **1** (0.255 g, 0.58 mmol) was added and the resultant mixture was stirred at room temperature overnight. The solvent was removed, and the resultant residue was dissolved in dichloromethane (100 ml)

which was washed with water (2 x 25 ml). The aqueous layers were re-extracted with 25 ml dichloromethane, and the combined organic layers dried over anhydrous $MgSO_4$, filtered, and dried in vacuo. The mixture was purified by column chromatography (elution with CH_2Cl_2/CH_3OH 95:5 v/v) to give the product as a white solid: ^{1}H NMR δ_H (400 MHz; $CDCl_3$) 5.13 (6H, s), 2.68 (6H, q, *J* = 7 Hz), 2.02 (9H, s), 1.70 (9H, 13 s), 0.78 (9H, t, *J* = 7Hz) ppm; ^{13}C RMN δ_C (75 MHz; $CDCl_3$) 145.1, 135.4, 130.2, 125.5, 116.9, + 44.9, 23.9, 14.3, 12.4, 9.6 ppm; MS (ESI): m/z calc. for [M + H] 723.08, found 723.08; mp 132°C.

Synthesis of 1,3,5-tris((4,5-dimethylimidazol-1-yl)methyl)-2,4,6-Triethylbenzene 5. (0.771 g, 54%) To a solution of 4,5-trimethyl-1*H*-imidazole **3** (1.13 g, 11.7 mmol) in acetonitrile (20 ml) was added dropwise a solution of 1 M NaOH (11.7 mmol), and the solution was stirred for 10 min. The 1,3,5-tris(bromomethyl)-2,4,6-triethylbenzene **1** (1.3 g, 2.95 mmol) was added and the resultant mixture was stirred overnight at room temperature. The solvent was removed, and the resultant residue was dissolved in dichloromethane (100 ml) which was washed with water (2 x 25 ml). The aqueous layers were re-extracted with 25 ml dichloromethane, and the combined organic layers dried over anhydrous $MgSO_4$, filtered, and dried in vacuo. Giving a pure white solid. ^{1}H RMN δ_H (300 MHz; $CDCl_3$) 6.71 (3H, s), 4.92 13 (6H, s), 2.54 (6H, q, J = 7.5 Hz), 2.22 (9H, s), 2.14 (9H, s), 0.95 (9H, t, J = 7.5 Hz) ppm; ^{13}C RMN δ_C (75 MHz; $CDCl_3$) 145.5, 134.1, 133.3, 130.3, 122.2, 43.0, 23.5, 15.2, 12.6, 8.7 ppm; MS (ESI): + m/z calc. for [M + H] 487.35, found 487.35; mp 160°C.

Synthesis of Tris-imidazolium receptor $6^{3+}\cdot 3Br^-$. (0.300 g, 42%) To a solution of tris-imidazole **4** (0.339 g, 0.47 mmol) in acetonitrile (150 ml) was added dropwise a solution of 9-(bromomethyl)anthracene (0.635 g, 2.3 mmol) in acetonitrile (50 ml) and the resultant mixture was stirred 5 days at room temperature. The volume of solvent was concentrated to 50 ml and diethyl ether (50 ml) was added. The resulting precipitate was collected and washed with diethyl ether. The crude obtained was purified by column chromatography (elution with CH_2Cl_2/CH_3OH (8:2 v/v) to give the desired tris-imidazolium receptor as bromide salt. ^{1}H NMR δ_H (300 MHz; CD_3CN/CD_3OD) 8.72 (3H, s), 8.14 (6H, d, J = 8 Hz), 8.04 (6H, d, J = 8 Hz), 7.64-7.58 (6H, m), 7.55-7.50 (6H, m), 6.39 (6H, s), 5.44 (6H, s), 2.54 (6H, q, J = 9 Hz), 1.77 (18H, s), 0.67 (9H, t, J = 9 Hz) ppm; ^{13}C NMR δ_C (75 MHz; CD_3CN/CD_3OD) 148.5, 132.7, 132.4, 132.1, 131.9, 131.1, 130.3, 129.2, 126.9, 124.3, 123.3, 121.2, 25.8, 15.3, 10.7, 10.5 ppm; MS (ESI): m/z calc. for $[M^{3+} + 2Br^-]^+$ 1457.17, found 1457.17; mp 192°C.

Synthesis of Tris-imidazolium receptor $6^{3+}\cdot 3PF_6^-$. (0.107 g, 95%) A solution of bis-imidazolium receptor as the bromide salt $\mathbf{6^{3+}\cdot 3Br^-}$ (0.100 g, 0.06 mmol) in CH_2Cl_2 (20 ml) was washed with a saturated solution of NH_4PF_6 in H_2O and stirred for 20 min (5 × 20 mL). The organic solvent was collected and dried with anhydrous Na_2SO_4. The solid was separated by filtration, and the solvent was removed under reduced pressure to give the hexafluorophosphate salt in quantitative yield. ^{1}H RMN δ_H (400 MHz; CD_3CN/CD_3OD) 8.75 (3H, s), 8.15 (6H, d, J = 8 Hz), 8.00 (6H, d, J = 8 Hz), 7.64-7.60 (6H, m), 7.58-7.53 (6H, m), 6.36 (6H, s), 5.34 (6H, s), 2.44 (6H, q), 1.84 (9H, s), 1.71 (9H, s), 0.65 (9H, t, J = 8 Hz) ppm; ^{13}C RMN δ_C (100 MHz; CD_3CN/CD_3OD) 148.4, 132.5, 132.2, 131.8, 131.8, 130.9, 130.0, 129.1, 126.70, 124.0, 122.9, 120.3, 49.1, 48.4, 25.4, 15.0, 10.5, 10.3 ppm; MS (ESI): m/z calc. for $[M^{3+} + 2PF_6^-]^+$ 1587.26, found 1587.26; mp. 213°C.

Synthesis of Tris-imidazolium receptor $7^{3+}\cdot 3PF_6^-$. (0.856 g, 36%) To a solution of tris-imidazole **5** (0.771 g, 1.58 mmol) in acetonitrile (150 ml) was added dropwise a solution of 9-(bromomethyl)anthracene (2.15 g, 7.9 mmol) in acetonitrile (50 ml) and the resultant mixture was stirred 5 days at room temperature. The volume of solvent was concentrated to 50 ml and diethyl ether (50 ml) was added. The resulting precipitate was collected and washed with diethyl ether. The crude obtained was purified by column chromatography (elution with $CH_3CN/H_2O/KNO_3$ (sat) (14:2:1 v/v). The organic solvent was removed and the pure compound was solved in H_2O layer. A saturated solution of NH_4PF_6 in H_2O was added and stirred for 20 min. The resulting precipitate was collected and washed with diethyl ether to give the tris-imidazolium receptor as hexafluorophosphate salt. ^{1}H RMN δ_H (400 MHz; CD_3CN/CD_3OD) 8.67 (3H, s), 8.11-8.08 (6H, m), 7.94-7.91 (6H, m), 7.53-7.49 (12H, m), 6.37 (3H, s), 5.97 (6H, s), 4.49 (6H, s), 2.42 (9H, s), 1.79 (6H, q, J = 8 Hz), 1.78 (9H, s), 0.15 (9H, t, J = 8 Hz) ppm; ^{13}C RMN δ_C (100 MHz; CD_3CN/CD_3OD) 149.0, 133.2, 133.1, 132.6, 132.5, 131.3, 130.9, 130.2, 129.7, 129.2, 127.5, 124.5, 122.8, 46.8, 45.8, 24.6, 16.1, 9.8, 9.3 ppm; MS (ESI): m/z calc. for $[M^{3+} + 2PF_6^-]$+ 1349.53, found 1349.53; mp 243°C.

Acknowledgements

We thank the government of the Spain Agencia Estatal de Investigación (AEI) and Fondo Europeo de Desarrollo Regional (FEDER, UE) projects CTQ2017-86775-P and CTQ2016-79345-P and Fundación Séneca Región de Murcia (CARM) projects 20819/PI/18 and 20789/PI/18 for financial support. P. S. and F.Z. also acknowledges the University of Murcia for a FPU predoctoral grant and a postdoctoral grant respectively.

Notes and references

1 L. Chen, S.N. Berry, X. Wu, E.N.W. Howe and P.A. Gale, *Chem.*, 2020, **6**, 61.
2 P. Molina, F. Zapata and A. Caballero, Chem. Rev., 2017, **117**, 9907.
3 N. H. Evans and P. D. Beer, *Angew. Chem., Int. Ed.*, 2014, **53**, 11716.
4 P. A. Gale, E. N. W. Howe and X. Wu, *Chem*, 2016, **1**, 351.
5 P. A. Gale and C. Caltagirone, *Chem. Soc. Rev.*, 2015, **44**, 4212.
6 P. A. Gale, N. Busschaert, C. J. E. Haynes, L. E. Karagiannidis and I. L. Kirby, *Chem. Soc. Rev.*, 2014, **43**, 205.
7 L. E. Santos-Figueroa, M. E. Moragues, E. Climent, A. Agostini, R. Martinez-Mañez and F. Sancenon, *Chem. Soc. Rev.*, 2013, **42**, 3489.
8 S. Kubik, *Chem. Soc. Rev.*, 2010, **39**, 3648.
9 F. P. Schmidtchen, M. Berger, *Chem. Rev.* 1997, **97**, 1609.
10 H. J. Schneider, *Angew. Chem. Int. Ed.* 2009, **48**, 3924.
11 J. M. Lehn, *Supramolecular chemistry concepts and perspectives*, Wiley-VCH, Weinheim, 1995.
12 J. W. Steed and J. L. Atwood, *Supramolecular chemistry*, Wiley, Chichester, 2000.
13 G. Gilli and P. Gilli, *The Nature of the Hydrogen Bon*d, Oxford University Press, Oxford, 2009.

14 G. R. Desiraju and T. Steiner, *The Weak Hydrogen Bond in Structural Chemistry and Biology*, Oxford, New York, 1999 .
15 S. Scheiner, *Hydrogen Bonding. A Theoretical Perspective*, Oxford University Press, New York, 1997.
16 S. J. Grabowski, *Hydrogen Bonding—New Insights*, Springer, Amsterdam, 2006.
17 G. Cavallo, P. Metrangolo, R. Milani, T. Pilati, A. Priimagi, G. Resnati and G. Terraneo, *Chem. Rev*., 2016, **116**, 2478.
18 P. Scilabra, G. Terraneo, G. Resnati, *Acc. Chem. Res.,* 2019*,* **52***,* 1313.
19 S. Scheiner, *Acc. Chem. Res*., 2013, **46**, 280.
20 A. Bauzá, T. J. Mooibroek and A. Frontera, *Angew. Chem. Int. Ed*., 2013, **52**, 12317.
21 A. Bauzá and A. Frontera, *Angew. Chem. Int. Ed.* 2015, **54**, 7340.
22 S. Grabowski, *J. Comput. Chem*., 2018, **39**, 472.
23 P. Politzer and J. S. Murray, *Crystals,* 2017, **7**, 212.
24 J. S. Murray, P. Lane, T. Clark, K. E. Riley and P. Politzer, *J. Mol. Model,* 2012, **18**, 541.
25 G. Cavallo, P. Metrangolo, R. Milani, T. Pilati, A. Primagi, G. Resnati and G. Terraneo, *Chem. Rev.*, 2016, **116**, 2478.
26 L. C. Gilday, S. W. Robinson, T. A. Barendt, M. J. Langton, B. R. Mullaney and P. D. Beer, *Chem. Rev.*, 2015, **115**, 7118.
27 L. González, F. Zapata, A. Caballero, P. Molina, C. Ramírez de Arellano, I. Alkorta and J. Elguero, *Chem. Eur. J.*, 2016, **22**, 7533.
28 F. Zapata, S. J. Benítez-Benítez, P. Sabater, A. Caballero and P. Molina, *Molecules*, 2017, **22**, 2273.
29 P. Sabater, F. Zapata, A. Caballero, N. de la Visitación, I. Alkorta, J. Elguero and P. Molina, *J. Org. Chem.*, 2016, **81**, 744.
30 F. Zapata, A. Caballero and P. Molina, *Eur. J. Inorg. Chem.*, 2017, 237.
31 W. L. Leong and J. J. Vittal, *Chem. Rev*., 2011, **111,** 688.
32 K. Otsubo, Y.Wakabayashi, J. Ohara, S. Yamamoto, H.Matsuzaki, H. Okamoto, K. Nitta, T. Uruga and H. Kitagawa, *Nat. Mater*., 2011, **10**, 291.
33 R. Chakrabarty, P. S. Mukherjee and P. J. Stang, *Chem. Rev*., 2011, **111**, 6810.
34 R. Kaminker, R. Popovitz-Biro and M. E. van der Boom, *Angew. Chem., Int. Ed*., 2011, **50**, 3224.
35 G. N. Newton, T. Onuki, T. Shiga, M. Noguchi, T. Matsumoto, J. S. Mathieson, M. Nihei, L. Cronin and H. Oshio, *Angew. Chem., Int. Ed.*, 2011, **50**, 4844.
36 J. Fan, M. L. Saha, B. Song, H. Schonherr and M. Schmittel, *J. Am. Chem. Soc.*, 2012, **134**, 150.
37 Q. Li, W. Zhang, O. S . Miljanic, C.-H. Sue, Y.-L. Zhao, L. Liu, C. B. Khobler, J. F. Stoddart and O. M. Yaghi, *Science*, 2009, **325**, 85.
38 D. Zhao, D. J. Timmons, D. Yuan and H.-C. Zhou, *Acc. Chem. Res*., 2011, **44**, 123
39 S. J. Loeb, *Chem. Soc. Rev*., 2007, **36**, 226..
40 G. J. E. Davidson, S. Sharma and S. J. Loeb, *Angew. Chem., Int. Ed*., 2010, **49**, 4938.
41 P. Wei, X. Yan and F. Huang, *Chem. Soc. Rev.*, 2015, **44**, 815.
42 A. Winter and U. S. Schubert, *Chem. Soc. Rev.*, 2016, **45**, 5311.
43 N. Busschaert, M. Wenzel, M. E. Light, P. I. Hernández, R. P. Tomás and P. A. Gale, *J. Am. Chem. Soc.*, 2011, **133**, 14136.
44 R. Custelcean, P. Remy, P. V. Bonnesen, D. Jiang and B. A. Moyer, *Angew. Chem., Int. Ed.*, 2008, **47**, 1866.
45 M. Arunachalam and P. Ghosh, *Chem. Commun.*, 2009, 5389.
46 M. Arunachalam and P. Ghosh, *Chem. Commun*., 2009, 3184.
47 I. Ravikumar, P. S. Lakshminarayanan, M. Arunachalam, E. Suresh and P. Ghosh, *Dalton Trans.*, 2009, 4160.
48 M. Arunachalam and P. Ghosh, *Cryst. Eng. Comm.*, 2010, **12**, 1621.
49 M. Arunachalam and P. Ghosh, *Inorg. Chem.*, 2010, **49**, 943.
50 I. Ravikumar and P. Ghosh, *Chem. Commun.*, 2010, **46**, 1082.
51 S. Kumar Dey, A. Basu, R. Chutia and G. Das. *RSC Adv.*, 2016, **6**, 26568.
52 U. Manna and G. Das, *New J. Chem.*, 2018, **42**, 19164.
53 F. Zapata, L. González, A. Caballero, A. Bastida, D. Bautista, and P. Molina. *J. Am. Chem. Soc.*, 2018, **140**, 2041.
54 K. Ghosh, D. Kar, S. Joardar, A. Samadder and A.R. Khuda-Bukhsh, *RSC Adv.*, 2014, **23**, 1190.
55 M. del Carmen Gonzalez, F. Oton, A. Espinosa, A. Tarraga and P. Molina, *Org. Biomol. Chem.*, 2015, **5**, 1429.
56 W. Li, J. Sun, J. Shi, S. Hao, Q. Liu and G. Yu, *Supramol. Chem.*, 2015, 686.
57 X. Zhuang, W. Liu, J. Wu, H. Zhang and P. Wang, *Spectrochim. Acta A*, 2011, **79**, 1352.
58 S. Biswas, M. Gangopadhyay, S. Barman, J. Sarkar and N.D.P. Singh, *Sens. Actuators B*, 2016, **222**, 823.
59 L. Zhao, G. Liu and B. Zhang, *Spectrochim. Acta A*, 2016, **169**, 45.
60 Y. Shiraishi, M. Nakamura, N. Matsushita and T. Hirai, *New J. Chem.*, 2016, **40**, 195.
61 A. Jain, R. Gupta and M. Agarwal, *J. Heterocycl. Chem.*, 2017, 54.
62 A. Jain, R. Gupta and M. Agarwal, *Anal. Chem. Lett.*, 2017, **7**, 170.
63 S. Chakraborty, R. Dutta and P. Ghosh, *Chem. Commun.*, 2015, *51*, 14793.
64 C. J. Serpell, N. L. Kilah, P. J. Costa, V. Felix and P. D. Beer, *Angew. Chem., Int. Ed,.* 2010, **49**, 5322.
65 A. D'Sa and L. A. Cohen, *J. Heterocycl. Chem.*, 1991, **28**, 1819.
66 A. Sorrenti, J. Leira-Iglesias, A. J. Markvoort, T. F. A de Greef and T. M. Hermans, *Chem. Soc. Rev*., 2017, **46**, 5476.
67 D. Zhao, J. Moore, *Org. Biomol. Chem*. 2003, **1**, 3471.
68 P. Kuzmic, *Anal. Biochem.*, 1996, **237**, 260.
69 G. Basu, M. Kubasik, D. Anglos, B. A. Secor and A. Kuki, *J. Am. Chem. Soc.*, 1990, **112**, 9410.
70 K. N. Solov'ev and E. A. Borisevich, *Phys.-Usp.,* 2005, **48**, 231
71 M. Rae, F. Perez-Balderas, C. Baleizao, A. Fedorov, J. A. S. Cavaleiro, A. C. Tome and M. N. Berberan-Santos, *J. Phys. Chem. B*, 2006, **110**, 12809.
72 F. Zapata, L. Gonzalez, A. Caballero, I. Alkorta, J. Elguero, P. Molina, *Chem. Eur. J.,* 2015, **21**, 9797.
73 I. Mata, I. Alkorta, E. Molins, E. Espinosa, *ChemPhysChem*, 2012, **13**, 1421.
74 I. Mata, I. Alkorta, E. Molins, E. Espinosa, *Chem. Phys. Lett.,* 2013, **555**, 106.